Chemistry of *C*-Trimethylsilyl-Substituted Heterocarboranes. 28. Selective Alkylation and Reactivity of "Carbons Adjacent" and "Carbons Apart" Tetracarba-*nido*-dodecaborane(12) Derivatives toward Group 1 and Group 2 Metals. Synthetic, Spectroscopic, and Structural Investigations on Lithium-, Sodium-, Potassium-, Cesium-, and Magnesium-Complexed C_4B_8 Carboranes

Narayan S. Hosmane,*[,†,‡,§] Hongming Zhang,[‡] John A. Maguire,*[,‡] Ying Wang,[‡] Temesgen Demissie,[‡,||] Thomas J. Colacot,[‡] Maria B. Ezhova,[‡] Kai-Juan Lu,[‡] Dunming Zhu,[‡] Thomas G. Gray,[‡] Sarah C. Helfert,[‡] Suneil N. Hosmane,[‡] Jess D. Collins,[‡] Frank Baumann,[⊥] Wolfgang Kaim,*[,⊥] and William N. Lipscomb*[,||]

Department of Chemistry and Biochemistry, Northern Illinois University, DeKalb, Illinois 60115, Department of Chemistry, Southern Methodist University, Dallas, Texas 75275, Department of Biophysics, Harvard University, Cambridge, Massachusetts 02138, and Institut für Anorganische Chemie, Universität Stuttgart, Pfaffenwaldring 55, 70569 Stuttgart, Germany

Received August 23, 1999

The "carbons apart" tetracarbon carborane *nido*-2,6-$(R)_2$-4,12-$(SiMe_3)_2$-2,4,6,12-$C_4B_8H_8$ (R = $SiMe_3$ (**I**), *n*-butyl (**II**)) and several of its B-alkylated derivatives react with Mg metal in THF solvent to produce magnesacarboranes (**IV**−**VI** and **XI**) in yields ranging from 57% to 74%. The magnesacarboranes were characterized by chemical analysis and infrared and ^1H, ^{11}B, and ^{13}C NMR spectroscopy and by single-crystal X-ray diffraction. Two types of cages were found, one in $(THF)_2Mg(SiMe_3)_4(B\text{-}Me)C_4B_7H_7$ (**IV**) and the other in $(L)_2Mg(SiMe_3)_2(R)_2(B\text{-}Y)C_4B_7H_7$ (L = THF, R = $SiMe_3$, Y = *t*-Bu (**V**); L = THF, R = $SiMe_3$, Y = H (**VI**); $(L)_2$ = TMEDA, R = *n*-Bu, Y = H (**XI**)). Both cages showed the presence of electron-precise C and B atoms, as well as electron-deficient fragments. Approximate density functional ab initio molecular orbital calculations showed that the dianionic C_4B_8 cage can exist in a number of energy-equivalent isomeric forms that can be trapped by a metal ion such as Mg. The reactions of **I** with the group 1 metals followed a different course in which two distinct steps occurred. The first step formed the paramagnetic intermediates which, in a slower step, reacted with a second equivalent of the metal to give the diamagnetic $[(SiMe_3)_4C_4B_8H_8]^{2-}$. For the lighter metals, this dianion picked up a proton to give the products $[(THF)_4M][(SiMe_3)_4C_4B_8H_9]$ (M = Li (**VIII**), Na (**IX**), K (**X**)) in 35−54% yield. In the case of Cs, no protonation occurred and the final product was a polymeric dicesiacarborane, $[exo\text{-}Cs(TMEDA)\text{-}1\text{-}Cs\text{-}(SiMe_3)_4C_4B_8H_8]_n$ (**VII**), isolated in 41% yield. All were characterized by chemical analysis and infrared and ^1H, ^{11}B, and ^{13}C NMR spectroscopy; **VII** and **VIII** were additionally characterized by single-crystal X-ray diffraction studies. In **VIII**−**X** the group 1 metal was solvated by four THF molecules and was not involved in the cage, while in **VII** one Cs occupied an apical position above a C_3B_3 open face of one carborane and bonded to a B_3 face of a neighboring carborane. The second Cs, solvated by a TMEDA molecule, occupies an exo-polyhedral position and was not part of the polymeric chain. One "carbons adjacent" magnesacarborane, $exo\text{-}(\mu\text{-}H)_3Mg(THF)_3(SiMe_3)_2(Me)_2C_4B_8H_8$ (**XII**), was also synthesized, in 81% yield, by the reaction of the metal with the $(SiMe_3)_2(Me)_2C_4B_8H_8$ precursor. Single-crystal X-ray diffraction studies showed the compound to be composed of an exo-polyhedral $[Mg(THF)_3]^{2+}$ that is loosely bound to a $[(SiMe_3)_2(Me)_2C_4B_8H_8]^{2-}$ cage. The carborane is best described as an 10-vertex *arachno*-$(SiMe_3)_2C_2B_8H_8$ cage that subtends an electron-precise MeC═CMe fragment.

Introduction

The carboranes with the general formula $R_4C_4B_8H_8$ (R = cage-carbon substituent) are of interest in that they constitute a class of neutral cage molecules with both a high carbon content and an enriched cage-electron count, both of which exert, sometimes conflicting, structural influences. Grimes and co-workers first reported on the syntheses, structures, and reactivities of

[†] Northern Illinois University.
[‡] Southern Methodist University.
[§] Address correspondence to Northern Illinois University.
[||] Harvard University.
[⊥] Universität Stuttgart.

10.1021/om990677z CCC: $19.00
Publication on Web 01/26/2000

several of these tetracarbon carboranes, all of which possessed the common structural feature that the cage carbons were localized on one side of very distorted icosahedral cages.[1−5] In one of these "carbons adjacent" isomers the carbon atoms were bonded contiguously in a Z-shaped pattern,[3] while in the other, the middle C−C bond was ruptured, leading to a more open structure.[4] However, the proximate locations of the cage carbons were maintained in all isomers. These "carbons adjacent" compounds were obtained as the products from the mild air oxidation of the metal−hydride complexes $(R_2C_2B_4H_4)_2MH_x$ (M = Fe ($x = 2$), Co ($x = 1$); R = CH_3, C_2H_5, *n*-C_3H_7, $CH_2C_6H_5$).[1,2,5] On the other hand, when the dianions [*nido*-2-($SiMe_3$)-3-(R)-2,3-$C_2B_4H_4$]$^{2-}$ (R = $SiMe_3$, *n*-Bu, *t*-Bu) were oxidized by $NiCl_2$, a completely different set of tetracarbon carboranes were produced.[6,7] In these trimethylsilyl-substituted compounds, the cage carbons were more evenly dispersed throughout the cage, being separated by at least one boron to give the so-called "carbons apart" compounds. One of these, *nido*-2,4,7,9-($SiMe_3$)$_4$-2,4,7,9-$C_4B_8H_8$, is of particular interest in that it is a 12-vertex cage whose structure is based more on a cuboctahedron than an icosahedron.[6,7] The other isomer, exemplified by *nido*-2,4,6,12-($SiMe_3$)$_4$-2,4,6,12-$C_4B_8H_8$, had a more traditional *nido* cage structure with an open C_3B_3 face surmounting a B_5 ring and an apical cage carbon. Most of the C_4B_8 carboranes exhibit nonrigid stereochemistry, showing multiple isomerization or fluxional behavior in solution.[1,4,6]

Both sets of carboranes can be reduced to give dianionic cages, which on metalation produced, at least formally, 13-vertex metallacarboranes. Grimes and coworkers have reported the syntheses of a large number of d-block metallacarboranes in the "carbons adjacent" system.[1,8−11] Multiple structures were found for a particular carborane and metal group. These were thought to arise from the metal coordination of the numerous isomers of the C_4B_8 dianions that were present in the reaction solutions. While the reports on the metallacarboranes derived from the "carbons adjacent" carboranes are fairly extensive, the only metallacarboranes in the "carbons apart" system that have been reported are those contained in our preliminary reports on [$(THF)_4Li$][($SiMe_3$)$_4C_4B_8H_9$], [*exo*-Cs(TMEDA)-1-Cs-2,4,7,9-($SiMe_3$)$_4$-2,4,7,9-$C_4B_8H_8$], and $(THF)_2$Mg-($SiMe_3$)$_4C_4B_8H_8$.[12,13] All show quite different structures that bear no apparent relation to one another. We report herein the details of the studies on these three compounds, as well as the extension to other group 1 and group 2 metallacarboranes. These results further demonstrate the extreme structural variability found in the metallacarboranes derived from the tetracarbon carboranes.

Experimental Section

Materials. The synthesis of *nido*-2-($SiMe_3$)-3-(R)-2,3-$C_2B_4H_6$ (R = $SiMe_3$, *n*-butyl)[6,14,15] and their subsequent conversion to *nido*-2,6-(R)$_2$-4,12-($SiMe_3$)$_4$-2,4,6,12-$C_4B_8H_8$ (R = $SiMe_3$ (**I**), *n*-butyl (**II**))[6] followed literature methods. Mineral oil free NaH (Aldrich) and *tert*-butyllithium (*t*-BuLi; 1.5 or 1.7 M solution in pentane obtained from Aldrich) were used as received. Prior to use, anhydrous $NiCl_2$ (Aldrich) was heated to 120 °C in vacuo to remove any trace quantities of moisture. Benzene, THF, and *n*-hexane were dried over $LiAlH_4$ and doubly distilled before use. *N*,*N*,*N*,*N*−Tetramethylethylenediamine (TMEDA; Aldrich) was distilled in vacuo and stored over sodium metal. Sodium, lithium, potassium, and cesium metals (Aldrich) were handled in a drybox, and magnesium metal, methyl iodide, and methyl triflate (Aldrich) were used as received.

Spectroscopic and Analytical Procedures. Proton, lithium-7, boron-11, and carbon-13 pulse Fourier transform NMR spectra at 200, 77.7, 64.2, and 50.3 MHz, respectively, were recorded on an IBM-200 SY multinuclear NMR spectrometer. Infrared spectra were recorded on a Nicolet Magna−550 FT-IR spectrophotometer. Elemental analyses were obtained from E+R Microanalytical Laboratory, Inc., Corona, NY.

EPR Spectra. Electron paramagnetic resonance (EPR) spectra were recorded in the X-band on a Bruker System ESP 300 equipped with a Bruker ER035 M gauss meter and an HP 5350B microwave counter.

Synthetic Procedures. Except where otherwise indicated, all operations were conducted in vacuo. Room-temperature and sub-room-temperature experiments were carried out in Pyrex glass round-bottom flasks of 100−250 mL capacity, containing magnetic stirring bars and fitted with high-vacuum Teflon valves. Nonvolatile substances were manipulated in either a drybox or evacuable glovebags under an atmosphere of dry nitrogen. All known compounds among the products were identified by comparing their infrared and/or NMR spectra with those of authentic samples.

Syntheses of ($SiMe_3$)$_4$(B-Me)$C_4B_7H_7$ (III) and $(THF)_2$Mg-($SiMe_3$)$_4$(B-Me)$C_4B_7H_7$ (IV). In a drybox, a 0.71 g (1.63 mmol) sample of *nido*-2,4,6,12-($SiMe_3$)$_4$-2,4,6,12-$C_4B_8H_8$ (**I**) and excess methyl triflate (CF_3SO_3Me) were transferred into a 250 mL reaction flask equipped with a magnetic stirring bar. The flask was then attached to a high-vacuum line, cooled to −196 °C, pumped to remove any residual N_2 gas, and then heated to 95 °C with constant stirring. After the mixture was stirred at 95 °C for 7 days, the unreacted methyl triflate was removed in vacuo to collect a pale yellow liquid, identified as($SiMe_3$)$_4$(B-Me)$C_4B_7H_7$ (**III**) (0.53 g, 1.2 mmol; 74% yield).

A THF solution (15−20 mL) of this liquid (compound **III**; 0.35 g, 0.78 mmol) was then poured, in vacuo, onto an excess quantity of finely cut Mg metal at 25 °C with constant stirring. The resulting heterogeneous mixture was then stirred for 2 days, during which time the color of the reaction mixture

(1) (a) Grimes, R. N. *Adv. Inorg. Chem. Radiochem.* **1983**, *26*, 55. (b) Maynard, R. B.; Grimes, R. N. *J. Am. Chem. Soc.* **1982**, *104*, 5983.
(2) (a) Maxwell, W. M.; Miller, V. R.; Grimes, R. N. *J. Am. Chem. Soc.* **1974**, *96*, 7116. (b) Maxwell, W. M.; Miller, V. R.; Grimes, R. N. *Inorg. Chem.* **1976**, *15*, 1343.
(3) Freyberg, D. P.; Weiss, R.; Sinn, E.; Grimes, R. N. *Inorg. Chem.* **1977**, *16*, 1847.
(4) Venable, T. L.; Maynard, R. B.; Grimes, R. N. *J. Am. Chem. Soc.* **1984**, *106*, 6187.
(5) Spencer, J. T.; Pourian, M. R.; Butcher, R. J.; Sinn, E.; Grimes, R. N. *Organometallics* **1987**, *6*, 335.
(6) Hosmane, N. S.; Colacot, T. J.; Zhang. H.; Yang, J.; Maguire, J. A.; Wang, Y.; Ezhova, M. B.; Franken, A.; Demissie, T.; Lu, K.-J.; Zhu, D.; Thomas, J. L. C.; Collins, J. D.; Gray, T. G.; Hosmane, S. N.; Lipscomb, W. N. *Organometallics* **1998**, *24*, 5294.
(7) Hosmane, N. S.; Zhang, H.; Maguire, J. A.; Wang, Y.; Colacot, T. J.; Gray, T. G. *Angew. Chem., Int. Ed. Engl.* **1996**, *35*, 1000.
(8) Maxwell, W. M.; Bryan, R. F.; Grimes, R. N. *J. Am. Chem. Soc.* **1977**, *99*, 4008.
(9) Maxwell, W. M.; Weiss, R.; Sinn, E.; Grimes, R. N. *J. Am. Chem. Soc.* **1977**, *99*, 4016.
(10) Grimes, R. N.; Pipal, J. R.; Sinn, E. *J. Am. Chem. Soc.* **1979**, *101*, 4172.
(11) Maxwell, W. M.; Grimes, R. N. *Inorg. Chem.* **1979**, *18*, 2174.
(12) Hosmane, N. S.; Zhang, H.; Wang, Y.; Lu, K.-J.; Colacot, T. J.; Ezhova, M. B.; Helfert, S. C.; Collins, J. D.; Maguire, J. A.; Gray, T. G. *Organometallics* **1996**, *15*, 2425.
(13) Hosmane, N. S.; Demissie, T.; Zhang, H.; Maguire, J. A.; Lipscomb, W. N.; Baumann, F.; Kaim, W. *Organometallics* **1998**, *17*, 293.
(14) Hosmane, N. S.; Sirmokadam, N. N.; Mollenhauer, M. N. *J. Organomet. Chem.* **1985**, *279*, 359.
(15) Hosmane, N. S.; Barreto, R. D. *Inorg. Synth.* **1992**, *29*, 89.

changed from pale yellow to an off-white turbid solution. After the mixture was filtered in vacuo and the residue on the frit was washed repeatedly with a 1:1 solvent mixture of *n*-hexane and benzene, a clear filtrate was obtained. Slow removal of the solvents from the filtrate afforded an off-white residue in the flask, which was further purified by recrystallization from a THF solution to afford a colorless crystalline solid, identified as $(THF)_2Mg(SiMe_3)_4(B\text{-}Me)C_4B_7H_7$ (**IV**; 0.32 g, 0.52 mmol; mp >250 °C), in 67% yield. Anal. Calcd for $C_{25}H_{62}B_8Si_4O_2Mg$ (**IV**): C, 48.60; H, 10.11. Found: C, 48.81; H 10.11. Spectroscopic data for compound **III**: ^{11}B NMR (C_6D_6, relative to external $BF_3{\cdot}OEt_2$) δ 7.84 (d, 4B; ^1J(BH) = 154 Hz, cage BH), 0.39 (s, 1B, cage BMe), −16.1 (d, 3B, ^1J(BH) = 154.1 Hz, cage BH). Spectroscopic data for compound **IV**: ^{1}H NMR (THF-d_8, relative to external Me_4Si) δ 3.86 (s, br, 8H, THF), 2.02 (s, br, 8H, THF), 1.54 (s, 3H, BMe), 0.37 (br, 18H, $SiMe_3$), 0.28 (br, 18H, $SiMe_3$); ^{11}B NMR (THF-d_8, relative to external $BF_3{\cdot}OEt_2$) δ −8.31 (d, br, 5B, ^1J(BH) unresolved, cage BH), −14.58 (s, br, 1B, cage BMe), −27.11 (d, 2B, ^1J(BH) = 121 Hz; cage BH); IR (cm^{-1}; THF vs THF) 2516 (vs) (ν(BH)).

Synthesis of $(THF)_2Mg(SiMe_3)_4(B\text{-}t\text{-}Bu)C_4B_7H_7$ (V). *nido*-2,4,6,12-$(SiMe_3)_4$-2,4,6,12-$C_4B_8H_8$ (**I**) is prepared by the reaction of $NiCl_2$ with the dianion [*nido*-2,3-$(SiMe_3)_2$-2,3-$C_2B_4H_4]^{2-}$, which is normally obtained by deprotonation of the corresponding neutral *nido*-carborane by a strong base such as *n*-BuLi or *t*-BuLi.[6] In the process of preparing $(SiMe_3)_4C_4B_8H_8$, *t*-BuLi decomposed and produced a viscous yellow liquid, along with $(SiMe_3)_4C_4B_8H_8$, in the same detachable U-trap held at 0 °C. Further reaction of the THF solution of this viscous liquid with an excess quantity of finely cut Mg metal at 25 °C, by the procedure employed for the synthesis of **IV**, permitted the isolation of a colorless crystalline solid, identified by X-ray analysis as $(THF)_2Mg(SiMe_3)_4(B\text{-}t\text{-}Bu)C_4B_7H_7$ (**V**). Except for the expected differences in the ^{1}H and ^{13}C NMR spectra on substituting a *t*-Bu for a Me group, the spectroscopic data of this compound was the same as those given above for **IV**. Anal. Calcd for $[C_{28}H_{68}B_8Si_4O_2Mg]{\cdot}0.5C_6H_6$ (**V**): C, 53.27; H, 10.24. Found: C, 53.33; H, 10.21.

Synthesis of $(THF)_2Mg(SiMe_3)_4C_4B_8H_8$ (VI). A 0.65 g (1.49 mmol) sample of *nido*-2,4,6,12-$(SiMe_3)_4$-2,4,6,12-$C_4B_8H_8$ (**I**) was dissolved in ∼30 mL of THF and reacted with excess Mg metal in vacuo. When it was mixed, the reaction solution first turned pale yellow and then slowly had an off-white turbid appearance as the mixture was stirred for 3 days. The reaction mixture was filtered in vacuo and the residue washed repeatedly with a hexane/benzene (15/85) mixture until a clear filtrate was obtained. After slow removal of the solvent, a pale orange-yellow residue remained, which was further recrystallized from a benzene/hexane (4/1) solution to give off-white platelike crystals, identified as $(THF)_2Mg(SiMe_3)_4C_4B_8H_8$ (**VI**; 0.67 g, 1.1 mmol, 74% yield; mp 195 °C). Anal. Calcd for $C_{24}H_{60}B_8Si_4O_2Mg$ (**VI**): C, 47.73; H, 10.01. Found: C, 47.86; H, 10.28. Spectroscopic data: ^{1}H NMR δ 3.53 (s, br, 8H, THF), 1.33 (s, br, 8H, THF), 0.56 (s, 9H, $SiMe_3$), 0.45 (s, 9H, $SiMe_3$), 0.24 (s, 9H, $SiMe_3$), 0.12 (s, 9H, $SiMe_3$); ^{11}B NMR δ −23.52 (d, overlapping, 3B, ^1J(BH) = unresolved, cage BH), −25.13 (d, overlapping, 3B, ^1J(BH) = unresolved, cage BH), −44.60 (d, 2B, ^1J(BH) = 135 Hz, cage BH); ^{13}C NMR δ 69.70 (t, CH_2, THF, ^1J(CH) = 147.6 Hz), 28.38 (t, CH_2, THF, ^1J(CH) = 133.0 Hz), 3.11 (s, 2C, cage carbons (SiCB)), 5.07 (q(br, overlapping), $SiMe_3$, ^1J(CH) = 119−120 Hz), 4.09 (q(br, overlapping), $SiMe_3$, ^1J(CH) = 119−120 Hz), −1.37 (s, 2C, cage carbons (SiCB)); IR (cm^{-1}; THF vs THF) 2510 (vs, br), 2358 (m, br) (ν(BH)).

Synthesis of $[exo\text{-}Cs(TMEDA)\text{-}1\text{-}Cs\text{-}(SiMe_3)_4C_4B_8H_8]_n$ (VII). A 0.46 g (1.06 mmol) sample of the tetracarbon carborane $(SiMe_3)_4C_4B_8H_8$ (**I**) was reacted with an excess quantity of cesium metal in dry THF (30 mL) at room temperature with constant stirring. The colorless heterogeneous mixture rapidly turned to bright yellow. After the mixture was stirred constantly for 10 days, it was filtered in vacuo and the residue washed repeatedly with a solvent mixture of *n*-hexane and benzene until a clear filtrate was collected. After slow removal of the solvents from the filtrate, a slightly off-white residue was obtained, which, when further purified by recrystallization from a 2:1 *n*-hexane/TMEDA mixture, produced transparent colorless crystals, identified as [*exo*-Cs(TMEDA)-1-Cs$(SiMe_3)_4$-$C_4B_8H_8]_n$ (**VII**; 0.352 g; 0.432 mmol; mp >260 °C), in 41% yield. Compound **VII** is soluble in polar solvents but is less soluble in nonpolar organic solvents. Anal. Calcd for $C_{22}H_{60}B_8Si_4N_2Cs_2$ (**VII**): C, 32.33; H, 7.40, N, 3.43. Found: C, 32.58; H, 7.58; N, 3.51. Spectroscopic data: ^{1}H NMR (C_6D_6, relative to external Me_4Si) δ 2.39 (s, 4H, CH_2, TMEDA), 2.21 (s, 12H, Me, TMEDA), 0.31 (s, 9H, $SiMe_3$), 0.13 (s, 9H, $SiMe_3$), 0.01 (s, 18H, $SiMe_3$); ^{11}B NMR (C_6D_6, relative to external $BF_3{\cdot}OEt_2$) δ −17.43 (d, 1B, ^1J(BH) = 141 Hz, cage BH), −29.03 (d, v br, 6B, ^1J(BH) = unresolved, cage BH), −42.51 (d, 1B, ^1J(BH) = 125 Hz, cage BH); ^{13}C NMR (C_6D_6, relative to external Me_4Si) δ 57.71 (t, CH_2, TMEDA, ^1J(CH) = 132 Hz), 45.82 (q, Me, TMEDA, ^1J(CH) = 133 Hz), 2.19 (s, 2C, cage carbons (SiCB)), 1.89 (q(br, overlapping), $SiMe_3$, ^1J(CH) = 120 Hz), 1.42 (q(br, overlapping), $SiMe_3$, ^1J(CH) = 122 Hz), 0.55 (q(br, overlapping), $SiMe_3$, ^1J(CH) = 119 Hz), −0.14 (s, 2C, cage carbons (SiCB)); IR (cm^{-1}; THF vs THF) 2556 (vs), 2375 (vs), 2294 (ms), 2227 (m) (ν(BH)).

Electron paramagnetic resonance (EPR) studies of the reaction showed that the appearance of the initial yellow color coincided with the generation of a paramagnetic intermediate, which reacted further with Cs to produce **VII**.

Syntheses of $[(THF)_4M][(SiMe_3)_4C_4B_8H_9]$ (M = Li (VIII), Na (IX), K (X)). Compounds **VIII**−**X** were synthesized using the same procedures and underwent the same general changes during the course of the syntheses. Therefore, the synthesis of $[(THF)_4Li][(SiMe_3)_4C_4B_8H_9]$ (**VIII**) will be outlined, with just the starting quantities and the yields of the syntheses of **IX** and **X** being summarized. A 0.41 g sample of **I** was reacted with an excess quantity of finely divided Li metal in dry THF. On mixing, the solution turned red-orange. Subsequent studies showed that this was due to a paramagnetic intermediate, presumably the $[(SiMe_3)_4C_4B_8H_8]^-$ monoanion, that initially forms. The solution slowly turned brown and produced an EPR-silent solid, which was purified by recrystallization from a benzene/hexane mixture (4/1) to give transparent crystals of $[(THF)_4Li][(SiMe_3)_4C_4B_8H_9]$ (**VIII**; 0.31 g, 0.94 mmol; 46% yield; mp 190 °C). Anal. Calcd for $C_{32}H_{77}B_8Si_4O_4$ (**VIII**): C, 52.53; H, 10.61. Found: C, 52.39; H, 10.52.

In like manner, 0.55 g (1.26 mmol) and 0.52 g (1.19 mmol) of **I** reacted with excess Na and K to give respectively $[(THF)_4M][(SiMe_3)_4C_4B_8H_9]$ (M = Na (**IX**), 0.33 g, 0.44 mmol, 35% yield, mp 240 °C; M = K (**X**), 0.45 g, 0.64 mmol, 54% yield, mp 250−255 °C). Anal. Calcd for $C_{32}H_{77}B_8Si_4O_4Na$ (**IX**): C, 51.40; H, 10.38. Found: C, 51.43; H, 10.44. Calcd for $C_{32}H_{77}B_8Si_4O_4K$ (**X**): C, 50.31; H, 10.16. Found: C, 50.69; H, 10.18.

Spectroscopic data (C_6D_6, relative to external Me_4Si (^{1}H and ^{13}C NMR) or $BF_3{\cdot}OEt_2$ (^{11}B NMR)) for compound **VIII**: ^{1}H NMR 3.87 (s, br, 16H, THF), 2.03 (s, br, 16H, THF), 0.40 (s, 9H, $SiMe_3$), 0.29 (s, 9H, SiMe), 0.17 (s, 18H, $SiMe_3$); ^{11}B NMR −24.59 (d, vbr, 6B, ^1J(BH) unresolved, cage BH), −42.53 (d, 1B, ^1J(BH) = 123 Hz, cage BH), −46.94 (d, 1B, ^1J(BH) = 133 Hz, cage BH); ^{13}C NMR 68.63 (t, CH_2, THF, ^1J(CH) = 148 Hz), 34.87 (d (br), cage CH, ^1J(CH) = 135 Hz), 25.18 (t, CH_2, THF, ^1J(CH) = 133.2 Hz), 2.64 (q (br, overlapping), $SiMe_3$, ^1J(CH) = 119.5 Hz), 2.17 (q (br, overlapping), $SiMe_3$ ^1J(CH) = 120 Hz), 0.14 (s, 1C, cage carbons (SiCB)), −0.82 (s, 2C, cage carbons (SiCB); ^{7}Li NMR (relative to external aqueous $LiNO_3$) −2.87 (s, br, exo-polyhedral cage Li); IR (cm^{-1}; C_6H_6 vs C_6H_6) 2652 (s), 2597 (m) (ν(BH)). Spectroscopic data for compound **IX**: ^{1}H NMR δ 3.84 (s, br, 16H, THF), 2.00 (s, br, 16H, THF), 0.26 (s, 9H, $SiMe_3$), 0.15 (s, 9H, $SiMe_3$), 0.06 (s, 18H, $SiMe_3$); ^{11}B NMR δ −24.34 (d, br, 6B, ^1J(BH) unresolved, cage BH), −41.07 (d, 1B, ^1J(BH) = 123.1 Hz, cage BH), −49.53 (d, 1B, ^1J(BH) = 140.7 Hz, cage BH); ^{13}C NMR δ 67.93 (t, THF, ^1J(CH) = 146.2 Hz), 25.94 (t, THF, ^1J(CH) = 131 Hz), 1.96 (q

Scheme 1. Syntheses of Tetracarbon Carborane Compounds of Group 1 and Group 2 Metals

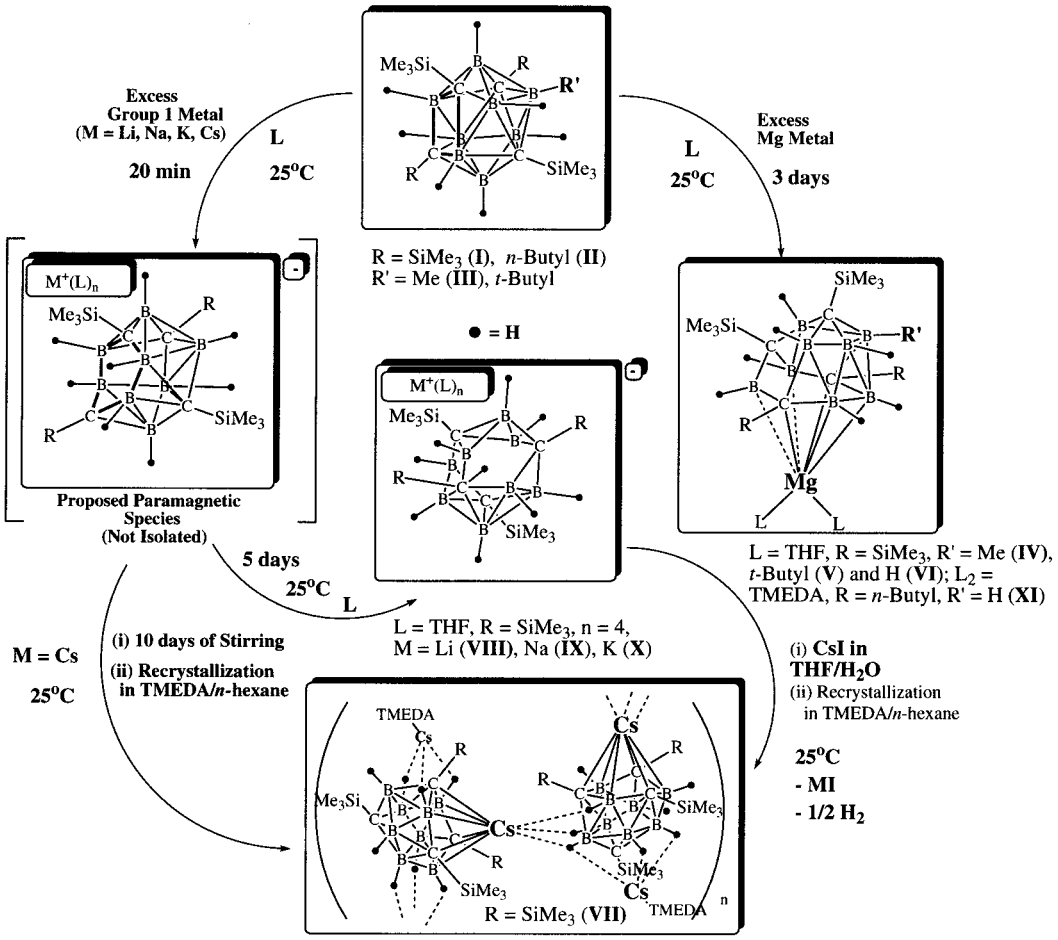

(br, overlapping), $SiMe_3$, $^1J(CH) = 119$ Hz), −0.45 (q (br, overlapping), $SiMe_3$, $^1J(CH) = 120$ Hz), −1.03 (q (br, overlapping), $SiMe_3$, $^1J(CH) = 120$ Hz), −1.21 (v br, 2C, cage carbons), −2.32 (v br, 2C, cage carbons); IR (cm^{-1}; C_6H_6 vs C_6H_6) 2655 (s), 2600 (m) (ν(BH)). Spectroscopic data for compound **X**: ^1H NMR δ 3.60 (s, br, 4H, THF), 1.61 (s, br, 4H, THF), 0.18 (s, br, 18H, $SiMe_3$), 0.11 (s, br, 18H, $SiMe_3$); ^{11}B NMR δ −22.3 (d, 6B, $^1J(BH) = 134.8$ Hz, cage BH), −36.2 (d, 1B, $^1J(BH) = 122$ Hz, cage BH), −47.1 (d, 1B, $^1J(BH) = 128.4$ Hz, cage BH); ^{13}C NMR δ 67.44 (t, THF, $^1J(CH) = 141$ Hz), 25.49 (t, THF, $^1J(CH) = 138$ Hz), 1.33 (q (br, overlapping), $SiMe_3$, $^1J(CH) = 121$ Hz), 0.68 (q (br, overlapping), $SiMe_3$, $^1J(CH) = 120$ Hz), 0.45 (q (br, overlapping), $SiMe_3$, $^1J(CH) = 121$ Hz), −0.75 (v br, 2C, cage carbons), −1.93 (v br, 2C, cage carbons); IR (cm^{-1}; THF vs THF) 2538 (ms), 2460 (m) (ν(BH)).

Synthesis of (TMEDA)Mg($SiMe_3$)$_2$(*n*-Bu)$_2$$C_4B_8H_8$ (XI). Using the same procedures described above for the synthesis of **VI**, a 0.47 g (1.17 mmol) sample of *nido*-2,6-(*n*-Bu)$_2$-4,12-($SiMe_3$)$_2$-2,4,6,12-$C_4B_8H_8$ was reacted in vacuo with an excess quantity of finely cut Mg in dry TMEDA at 25 °C to produce (TMEDA)Mg($SiMe_3$)$_2$(*n*-Bu)$_2$$C_4B_8H_8$ (**XI**; 0.35 g, 0.67 mmol; 57% yield; mp 200 °C). Anal. Calcd for $C_{24}H_{60}B_8Si_2N_2Mg$ (**XI**): C, 52.73; H, 11.06; N, 5.12. Found: C, 52.36; H, 10.94; N, 5.28. Spectroscopic data (C_6D_6, relative to external Me_4Si (^1H and ^{13}C NMR) or BF_3·OEt_2 (^{11}B NMR)) for compound **XI**: ^1H NMR δ 2.11 (s, 4H, TMEDA), 2.00 (s, 12H, TMEDA), 1.38 (s, 2H, *n*-Bu), 1.03 (s (br), 4H, *n*-Bu), 0.99 (s, 3H, Me(*n*-Bu)), 0.29 (s, 9H, $SiMe_3$), 0.22 (s, 9H, $SiMe_3$); ^{11}B NMR δ −4.32 (d (br), 3B, $^1J(BH)$ unresolved, cage BH), −14.45 (d (br), 3B, $^1J(BH)$ unresolved, cage BH), −25.52 (d (br), 2B, $^1J(BH)$ unresolved, cage BH); ^{13}C NMR δ 55.96 (t, TMEDA, $^1J(CH) = 136.5$ Hz), 43.58 (q, Me, TMEDA, $^1J(CH) = 134.2$ Hz), 35.42 (t, *n*-Bu, $^1J(CH) = 126$ Hz), 31.92 (t, *n*-Bu, $^1J(CH) = 123.4$ Hz), 23.68 (t, *n*-Bu, $^1J(CH) = 127.6$ Hz), 14.29 (q, Me(*n*-Bu), $^1J(CH) = 124$ Hz), 5.23 (q, $SiMe_3$, $^1J(CH) = 120$ Hz), 4.86 (s, cage carbons (SiCB)), 1.44 (s, cage carbons (CCB)); IR (cm^{-1}; C_6D_6 vs C_6D_6) 2513 (s), 2289 (m) (ν(BH)).

Synthesis of *exo*-(μ-H)$_3$Mg(THF)$_3$($SiMe_3$)$_2$(Me)$_2$$C_4B_8H_8$ (XII). A 0.60 g (1.88 mmol) sample of the "carbons adjacent" tetracarbon carborane *nido*-($SiMe_3$)$_2$(Me)$_2$$C_4B_8H_8$[6] was reacted in vacuo with an excess quantity of finely cut Mg metal in dry THF at 25 °C, with constant stirring. After the reaction mixture was stirred for 10 days, the usual filtration and workup procedures were carried out to isolate a pale yellow solid, which when further purified by recrystallization from 2:1 mixture of THF/benzene produced air-sensitive, transparent colorless crystals, identified as *exo*-(μ-H)$_3$Mg(THF)$_3$($SiMe_3$)$_2$-(Me)$_2$$C_4B_8H_8$ (**XII**; 0.58 g, 1.52 mmol; mp 78−80 °C) in 81% yield. Anal. Calcd for $C_{16}H_{40}B_8Si_2OMg$ (**XII**): C, 46.26; H, 9.71. Found: C, 46.34; H, 9.88. Spectroscopic data (THF-d_8, relative to external Me_4Si (^1H and ^{13}C NMR) or BF_3·OEt_2 (^{11}B NMR)) for compound **XII**: ^1H NMR δ 4.15 (s (br), 12H, THF), 2.31 (s (br),12H, THF), 2.67 (s, 6H, C_{cage}-Me), 0.38 (s, 18H, $SiMe_3$); ^{11}B NMR δ −2.08 (d(br), 5B, $^1J(BH)$ unresolved), −25.01 (d, 2B, $^1J(BH) = 111.1$ Hz), −29.33 (d (br), 1B, $^1J(BH)$ unresolved); ^{13}C NMR δ 71.37 (t, THF, $^1J(CH) = 147$ Hz), 63.43 (s (br), cage carbons), 29.06 (t, THF, $^1J(CH) = 135$ Hz), 24.84 (q, C_{cage}-Me, $^1J(CH) = 130$ Hz), 4.96 (q (br, overlapping), $SiMe_3$, $^1J(CH) = 120$ Hz), 4.90 (q (br, overlapping), $SiMe_3$, $^1J(CH) = 120$ Hz), 3.35 (s, cage carbons); IR (cm^{-1}; THF vs THF) 2560 (vs), 2544 (s) (ν(BH)).

EPR Spectroscopy during the Formation of [(THF)$_4$Li]-[($SiMe_3$)$_4$$C_4B_8H_9$] (VIII) and [*exo*-Cs(TMEDA)-1-Cs-(Si-Me$_3$)$_4$$C_4B_8H_8$]$_n$ (VII). As summarized in Scheme 1, the reduction of ($SiMe_3$)$_4$$C_4B_8H_8$ (**I**) with lithium metal in THF resulted in an orange solution which exhibits an EPR spectrum

($g = 2.0030$) with distinct hyperfine structure (see Figure 8). EPR spectra simulation was possible, assuming the coupling of four equivalent boron nuclei in natural isotopic distribution (80.2% ^{11}B, $I = {}^3/_2$; 19.8% ^{10}B, $I = 3$; $m(^{11}B)/m(^{10}B) = 2.99$). Coupling constants are 1.165 mT for $a(^{11}B)$ and 0.390 mT for $a(^{10}B)$; other hyperfine coupling exceeding the line width of 0.30 mT was not observed. These EPR results suggest a partial localization of spin in the reduced C_4B_8 skeleton of $(SiMe_3)_4C_4B_8H_8$; the other four boron nuclei seem to be situated in a nodal position of the singly occupied MO. In the absence of a structure of the radical intermediate, we cannot offer further interpretation. However, the symmetry and size of the boron hyperfine coupling are similar to those found in π type radicals.

The reaction of $(SiMe_3)_4C_4B_8H_8$ (**I**) with cesium also gave a paramagnetic orange solution; however, the partially resolved EPR spectrum observed ($g = 2.0030$) was best fitted assuming the coupling of two boron nuclei ($a(^{11}B) = 0.89$ mT, $a(^{10}B) = 0.30$ mT) and one cesium ($a(^{133}Cs) = 0.36$ mT; $I = {}^7/_2$, 100% natural abundance) with the unpaired electron. Among the stable alkali-metal isotopes, the ^{133}Cs nucleus has the highest hyperfine coupling constant, which would explain its coupling to a carborane radical in an ion-pair arrangement.

Calculations. Approximate density functional (DFT) ab initio molecular orbital calculations at several different levels of theory were carried out on either a Dec-αA or Silicon Graphics Indigo2 RS10000 workstation, using the Gaussian 94 series of programs.[16] Most calculations were carried out on model compounds having the same cage structures as the metallacarboranes found in this study, but with hydrogens being used in place of the cage carbon substituents. In most cases the geometries of the model compounds were optimized using Becke's three-parameter hybrid methods[17] and the correlation functional of Lee, Yang, and Parr[18] (B3LYP) at the 6-31G* or the 6-311G* levels of theory, starting with the X-ray positions of the heavy atoms. Boron-11 NMR chemical shifts were obtained using gauge-independent atomic orbital (GIAO)[19] calculations at the B3LYP/6-311G** level on the optimized structures. Such calculations have been found to give reliable ^{11}B NMR chemical shifts in a number of carboranes and metallacarboranes.[6,20,21] The ^{11}B NMR chemical shifts are relative to the $BF_3{\cdot}OEt_2$ standard. In all cases the standard was subjected to the same optimization/GIAO cycle as the particular compound.

Crystal Structure Analyses of $(THF)_2Mg(SiMe_3)_4(B\text{-}Me)C_4B_7H_7$ (IV), $(THF)_2Mg(SiMe_3)_4(B\text{-}t\text{-}Bu)C_4B_7H_7$ (V), $(THF)_2Mg(SiMe_3)_4C_4B_8H_8$ (VI), $[exo\text{-}Cs(TMEDA)\text{-}1\text{-}Cs(SiMe_3)_4C_4B_8H_8]_n$ (VII), $[(THF)_4Li][(SiMe_3)_4C_4B_8H_9]$ (VIII), $(TMEDA)Mg(SiMe_3)_2(n\text{-}Bu)_2C_4B_8H_8$ (XI), and $exo\text{-}(\mu\text{-}H)_3Mg(THF)_3(SiMe_3)_2(Me)_2C_4B_8H_8$ (XII). Suitable crystals of **IV**−**VIII**, **XI**, and **XII** were coated with epoxy resin and mounted sequentially on a Siemens R3m|V diffractometer. Final unit cell parameters, provided in Table 1, were obtained by a least-squares fit of the angles of 24 accurately centered reflections, and intensity data were collected at 220−230 K in the range $3.5 \le 2\theta \le 42-44°$ (**IV**−**VII**) or $3.0 \le 2\theta \le 46°$ (**VIII**, **XI**, and **XII**) using graphite-monochromatized Mo Kα radiation. Compound **VII** is chiral, and its structure was refined with a Flack parameter of −0.1(1). The particulars of the data collection and refinement are also listed in Table 1. All structures were solved by direct methods, and full-matrix least-squares refinements were performed using the SHELXTL-Plus package of programs.[22] Selected bond lengths and bond angles for all these compounds are listed in Table 2.

Results and Discussion

Syntheses. The monomethylated "carbons apart" carborane $(SiMe_3)_4(B\text{-}Me)C_4B_7H_7$ (**III**) was obtained in 74% yield from the reaction of **I** with neat methyl triflate. The general procedure followed was that described by Hawthorne and co-workers for the synthesis of permethylated 1,12-dicarba-*closo*-dodecaborane(12), $1,12\text{-}(CR)_2B_{10}(CH_3)_{10}$ (R = CH_3, H),[23] and by Michl et al. for the $[CB_{11}(CH_3)_{12}]^-$ monoanion.[24] The fairly high yield in this reaction, 74%, indicates that the addition of a single methyl moiety deactivates the cage for further methylation. Despite the presence of four $SiMe_3$ groups and increase in bulkiness of the cage upon monomethylation, the failure to methylate the cage further may not be simply due to steric effects; the other factors could be operating simultaneously during the alkylation.

All metallacarboranes in this study were synthesized by the reaction of the particular neutral tetracarbon carborane with excess metal in nonaromatic solvents, such as THF or TMEDA (Scheme 1). The magnesacarboranes **IV**−**VI**, **XI**, and **XII** were produced in moderate yields, ranging from 57% for **XI** to 81% for **XII**. The yields for the group 1 metallacarboranes were lower, being in the 41−54% range. These are unmaximized yields for the recrystallized products and may reflect solubility loss rather than competing or incomplete reactions; the main emphasis in this study was product structure, not synthetic efficiency. The formation of the magnesacarboranes seem to involve a direct transfer of the valence electrons from the magnesium to the carborane cage without the formation of an intermediate. However, that is not the case with the group 1 metallacarboranes. These cage reductions go in two distinct steps, the first involving the rapid formation of a paramagnetic intermediate, presumably the $[(SiMe_3)_4C_4B_8H_8]^-$ monoanion, which is then further reduced to the diamagnetic $[(SiMe_3)_4C_4B_8H_8]^{2-}$. Although the paramagnetic intermediate could not be isolated or structurally characterized, EPR simulations show that the intermediate found in the formation of the cesiacarborane (**VII**) may be different from that for the lithiacarborane (**VIII**). With cesium, the best simulation was for a species in which two boron atoms and a Cs were coupled with the unpaired electron. On the other hand, the intermediate in the lithium interaction with the C_4B_8 cage was consistent with a structure in which the unpaired electron couples with four equivalent borons, with the size of the hyperfine coupling being suggestive of a π-type radical. Since the solid-state structures of **VII** and **VIII** are quite different, they could well go through different intermediates. However, given the fact

(16) Frisch, M. J.; Trucks, G. W.; Schlegel, H. B.; Gill, P. M. W.; Johnson, B. F. G.; Robb, M. A.; Cheeseman, J. R.; Keith, T.; Peterson, G. A.; Montgomery, J. A.; Raghavachari, K.; Al-Laham, M. A.; Zakrzewski, V. G.; Ortiz, J. V.; Foresman, J. B.; Peng, C. Y.; Ayala, P. Y.; Chen, W.; Wong, M. W.; Andres, J. L.; Replogle, E. S.; Gomperts, R.; Martin, R. L.; Fox, D. J.; Binkley, J. S.; Defrees, D. J.; Baker, J.; Stewart, J. P.; Head-Gordon, M.; Gonzalez, C.; Pople, J. A. Gaussian 94, Revisions B.3 & E.2; Gaussian, Inc., Pittsburgh, PA, 1995.
(17) Becke, A. D. *J. Chem. Phys.* **1993**, *98*, 5648.
(18) Lee, C.; Yang, W.; Parr, R. G. *Phys. Rev.* **1988**, *B 37*, 785.
(19) Wolinski, K.; Hilton, J. F.; Pulay, P. *J. Am. Chem. Soc.* **1990**, *112*, 8251.
(20) (a) Ezhova, M. B.; Zhang, H.; Maguire, J. A.; Hosmane, N. S. *J. Organomet. Chem.* **1998**, *550*, 409. (b) Hosmane, N. S.; Lu, K.-J.; Zhang, H.; Maguire, J. A. *Organometallics* **1997**, *16*, 5163.
(21) Cheeseman, J. R.; Trucks, G. W.; Keith, T. A.; Frisch, M. J. *J. Chem. Phys.* **1996**, *104*, 5497.
(22) Sheldrick, G. M. Structure Determination Software Programs; Siemens X-ray Analytical Instrument Corp., Madison, WI, 1991.
(23) Jiang, W.; Knobler, C. B.; Mortimer, M. D.; Hawthorne, M. F. *Angew. Chem., Int. Ed. Engl.* **1995**, *34*, 1332.
(24) King, B. T.; Janousek, Z.; Grüner, B.; Trammell, M.; Noll, B. C.; Michl, J. *J. Am. Chem. Soc.* **1996**, *118*, 3313.

Table 1. Crystallographic Data[a] for Metalla-C_4B_8 Carboranes

(A) Compounds **IV**−**VIII**

	IV	V	VI	VII	VIII
formula	$C_{25}H_{62}B_8O_2Si_4Mg$	$C_{28}H_{68}B_8O_2Si_4Mg\cdot {}^1/_2C_6H_6$	$C_{24}H_{60}B_8O_2Si_4Mg$	$C_{22}H_{60}B_8N_2Si_4Cs_2$	$C_{32}H_{77}B_8O_4Si_4Li$
fw	617.9	699.0	603.9	817.4	731.7
space group	$P2_1/c$	$P\bar{1}$	$Pbca$	$P2_12_12_1$	$Pca2_1$
a, Å	10.309(2)	10.807(3)	14.821(4)	13.517(3)	21.449(4)
b, Å	33.730(7)	11.413(3)	18.685(7)	15.902(4)	10.809(2)
c, Å	11.617(3)	19.552	27.528(8)	18.927(4)	20.900(3)
α, deg		78.98(2)			
β, deg	111.13(2)	77.89(2)			
γ, deg		71.17(2)			
V, Å^3	3768(2)	2209(2)	7619(6)	4068.3(16)	4845.6(14)
Z	4	2	8	4	4
D_{calcd}, g cm^{-3}	1.089	1.051	1.053	1.334	1.002
abs coeff, mm^{-1}	0.196	0.174	0.193	1.925	0.152
crystal dimens, mm	0.30 × 0.35 × 0.15	0.30 × 0.25 × 0.15	0.35 × 0.20 × 0.15	0.30 × 0.35 × 0.35	0.15 × 0.30 × 0.25
scan type	ω	ω	ω	$2\theta-\theta$	ω
2θ range, deg	3.5−42.0	3.0−42.0	3.5−40	3.5−44.0	3.5−44.0
T, K	220	220	230	228	220
decay, %	0	0	0	0	0
no. of data collected	4322	5062	5301	2775	3082
no. of obsd rflns, $F > 6.0\sigma(F)$	2806	3650	1619	1423	1550
no. of params refined	383	432	353	193	401
GOF	1.36	1.48	1.19	2.46	2.14
$\Delta\rho_{max,min}$, e/Å^3	0.37, −0.29	0.31, −0.30	0.24, −0.24	1.6, −1.4	0.61, −0.23
R^b	0.048	0.042	0.055	0.096	0.076
$R_w{}^c$	0.061	0.060	0.060	0.121	0.093

(B) Compounds **XI** and **XII**

	XI	XII		XI	XII
formula	$C_{30}H_{57}B_8N_2Si_2Mg$	$C_{24}H_{56}B_8O_3Si_2Mg$	scan type	ω	$2\theta-\theta$
fw	612.7	559.7	2θ range, deg	3.5−42.0	3.0−46.0
cryst syst	monoclinic	monoclinic	T, K	230	228
space group	$P2_1/n$	$P2_1/c$	decay, %	0	0
a, Å	14.633(3)	9.973(10)	no. of data collected	4530	5043
b, Å	16.672(3)	21.190(2)	no. of obsd rflns, $F > 6.0\sigma(F)$	2425	3187
c, Å	16.970(3)	16.514(10)			
β, deg	102.860(10)	102.180(10)	no. of params refined	390	368
V, Å^3	4040.9(15)	3411.3(5)	GOF	1.75	1.72
Z	4	4	$\Delta\rho_{max,min}$, e/Å^3	0.47, −0.29	0.25, −0.32
D_{calcd}, Mg m^{-3}	1.007	1.090	R^b	0.063	0.054
abs coeff, mm^{-1}	0.124	0.146	R_w	0.079	0.077
cryst dimens, mm	0.25 × 0.35 × 0.15	0.40 × 0.30 × 0.25			

[a] Graphite-monochromated Mo Kα radiation, λ = 0.710 73 Å. [b] $R = \Sigma||F_o| - |F_c||/\Sigma|F_o|$; $R_w = [\Sigma w(F_o - F_c)^2/\Sigma w(F_o)^2]^{1/2}$. [c] $w = 1/[\sigma^2(F_o) + 0.001(F_o)^2]$.

that the starting carboranes and, presumably, the final products are stereochemically nonrigid, it is not unreasonable to assume that the intermediates could exist in more than one isomeric form, which would make characterization difficult. When the *n*-Bu-substituted carborane *nido*-2,6-(*n*-C_4H_9)$_2$-4,12-($SiMe_3$)$_2$-2,4,6,12-$C_4B_8H_8$ was reacted with excess Li, Na, K, or Cs, under conditions equivalent to those described for **VII**−**X**, the same color changes as seen in the formations of **VII**−**X** were observed. In addition, the final products were of the form [(THF)$_4$M][(*n*-Bu)$_2$($SiMe_3$)$_2$$C_4B_8H_9$] (M = Cs, Li, Na, K) which are equivalent to those found for **VII**−**X**. Thus, the reaction sequences seem to be general ones, with the Cs−carborane interactions being especially strong.

Structures. The solid-state structures of compounds **IV**−**VIII**, **XI,** and **XII**, as determined by single-crystal X-ray diffraction, are shown in Figures 1−7, respectively. Values of some important interatomic distances and bond angles are shown in Table 2; more complete listings of bond distances and angles are included in the Supporting Information.

The solid-state structure of (THF)$_2$Mg($SiMe_3$)$_4$$C_4B_8H_8$ (**VI**) was presented in our preliminary report on the formation of the first "carbons apart" C_4B_8 metallacarboranes (also see Figure 5).[12] The magnesacarboranes **V** and **XI** have cage structures that are essentially the same as that of **VI**, except that one of the borons in each is alkylated. This does not seem to materially affect the cage geometry. A comparison of the equivalent C_4B_8 intercage distances in **V**, **VI**, and **XI**, listed in Table 2, shows agreement to within ±0.013 Å, with the largest differences, ±0.027 and ±0.025 Å, occurring in the B(12)−B(22) and C(18)−B(22) distances, respectively.[25] All structures show that a magnesium ion, solvated by either two THF molecules (**V** and **VI**) or one TMEDA molecule (**XI**), is bonded symmetrically to four adjacent atoms (C(11), B(15), B(16) and C(17)) on a seven-member open face (C(14), B(13), C(11), B(15), B(16), C(17), and B(20)). For compound **VI**, the relevant bond distances are Mg−C(11) = 2.315(10) Å, Mg−B(15) = 2.393(12) Å, Mg−B(16) = 2.402(11) Å, and Mg−

(25) Whenever an average value of a parameter is given, the indetermination is listed in the average deviation.

Table 2. Selected Bond Lengths (Å) and Bond Angles (deg) for the Metalla-C_4B_8 Carboranes IV−VIII, XI, and XII

Bond Lengths (Å)

			Compound **IV**				
Mg−Si(3)	3.172(2)	Si(2)−C(14)	1.907(5)	C(14)−B(20)	1.668(8)	C(18)−B(19)	1.697(7)
Mg−C(11)	2.178(4)	Si(3)−C(16)	1.897(4)	B(15)−C(16)	1.635(6)	C(18)−B(21)	1.673(7)
Mg−B(12)	2.686(6)	Si(4)−C(18)	1.919(5)	B(15)−B(20)	1.839(8)	B(19)−C(19)	1.594(7)
Mg−B(13)	2.650(5)	C(11)−B(12)	1.512(8)	B(15)−B(22)	1.824(10)	B(19)−B(20)	1.784(8)
Mg−C(16)	2.182(5)	C(11)−B(13)	1.496(7)	C(16)−B(17)	1.634(8)	B(19)−B(21)	1.780(9)
Mg−B(17)	2.910(7)	B(12)−C(18)	1.590(8)	C(16)−B(22)	1.618(7)	B(20)−B(21)	1.743(9)
Mg−O(51)	2.030(3)	B(13)−C(14)	1.602(8)	B(17)−C(18)	1.712(7)	B(20)−B(22)	1.776(7)
Mg−O(61)	2.029(4)	C(14)−B(15)	1.725(6)	B(17)−B(21)	1.841(7)	B(21)−B(22)	1.778(8)
Si(1)−C(11)	1.848(5)	C(14)−B(19)	1.665(8)	B(17)−B(22)	1.825(8)		
			Compound **V**				
Mg−C(11)	2.315(3)	Si(2)−C(17)	1.898(4)	B(13)−C(14)	1.551(5)	C(17)−B(21)	1.759(4)
Mg−B(13)	2.664(4)	Si(3)−C(14)	1.876(4)	C(14)−B(19)	1.577(6)	C(18)−B(19)	1.595(5)
Mg−B(15)	2.375(4)	Si(4)−C(18)	1.896(3)	C(14)−B(20)	1.579(6)	C(18)−B(21)	1.697(6)
Mg−B(16)	2.366(5)	C(11)−B(12)	1.717(5)	B(15)−B(16)	1.789(6)	C(18)−B(22)	1.758(5)
Mg−C(17)	2.362(4)	C(11)−B(13)	1.547(5)	B(15)−B(22)	1.755(5)	B(19)−B(20)	1.999(5)
Mg−B(20)	2.685(4)	C(11)−B(15)	1.670(6)	B(16)−C(17)	1.659(5)	B(19)−B(21)	2.026(7)
Mg−O(51)	2.039(3)	B(12)−B(15)	1.773(5)	B(16)−B(21)	1.768(5)	B(21)−B(22)	1.791(5)
Mg−O(61)	2.032(3)	B(12)−C(18)	1.652(5)	B(16)−B(22)	1.789(5)	B(22)−C(43)	1.627(6)
Si(1)−C(11)	1.883(3)	B(12)−B(22)	1.812(7)	C(17)−B(20)	1.542(6)		
			Compound **VI**				
Mg−C(11)	2.315(10)	Si(2)−C(17)	1.886(9)	B(13)−C(14)	1.568(15)	C(17)−B(20)	1.555(16)
Mg−B(13)	2.644(12)	Si(3)−C(14)	1.865(10)	C(14)−B(19)	1.602(15)	C(17)−B(21)	1.762(14)
Mg−B(15)	2.393(12)	Si(4)−C(18)	1.878(10)	C(14)−B(20)	1.573(17)	C(18)−B(19)	1.540(15)
Mg−B(16)	2.402(11)	C(11)−B(12)	1.694(15)	B(15)−B(16)	1.813(16)	C(18)−B(21)	1.710(15)
Mg−C(17)	2.326(9)	C(11)−B(13)	1.550(15)	B(15)−B(22)	1.719(16)	C(18)−B(22)	1.698(15)
Mg−B(20)	2.687(14)	C(11)−B(15)	1.683(14)	B(16)−C(17)	1.649(14)	B(19)−B(20)	2.065(17)
Mg−O(51)	2.034(7)	B(12)−B(15)	1.749(16)	B(16)−B(21)	1.796(16)	B(19)−B(21)	2.064(16)
Mg−O(61)	2.027(8)	B(12)−C(18)	1.647(16)	B(16)−B(22)	1.772(16)	B(21)−B(22)	1.776(16)
Si(1)−C(11)	1.871(10)	B(12)−B(22)	1.734(17)				
			Compound **VII**				
Cs(1)−C(11)	3.585(36)	Cs(2)−B(15)	3.703(48)	C(11)−B(18)	1.716(73)	B(15)−B(19)	1.775(70)
Cs(1)−C(12)	2.954(43)	Cs(2)−B(19)	3.528(47)	C(11)−B(19)	1.790(63)	B(15)−B(20)	1.501(66)
Cs(1)−C(13)	3.506(50)	Cs(2)−B(20)	3.754(43)	C(12)−B(15)	1.612(65)	B(16)−B(20)	1.641(69)
Cs(1)−B(15)	3.526(48)	Cs(2)−C(34)	3.637(38)	C(12)−B(16)	1.657(65)	B(16)−B(21)	1.795(71)
Cs(1)−B(16)	3.561(52)	Cs(2)−N(51)	3.175(55)	C(12)−B(20)	1.499(61)	B(17)−B(18)	1.902(87)
Cs(1)−B(17)	3.318(59)	Cs(2)−N(52)	3.639(72)	C(13)−B(16)	1.859(69)	B(17)−B(22)	1.860(74)
Cs(1)−C(33)	3.475(44)	Cs(2)−C(32A)	3.906(40)	C(13)−B(17)	1.553(79)	B(18)−B(19)	1.851(79)
Cs(1)−C(36)	3.454(46)	Si(1)−C(11)	1.892(40)	C(13)−B(21)	1.766(75)	B(18)−B(22)	1.846(76)
Cs(1)−C(39)	3.641(58)	Si(2)−C(12)	1.800(41)	C(13)−B(22)	1.786(65)	B(19)−B(20)	1.829(63)
Cs(1)−B(16A)	3.441(52)	Si(3)−C(13)	1.760(56)	C(14)−B(18)	1.454(79)	B(20)−B(21)	1.977(65)
Cs(1)−B(20A)	3.729(45)	Si(4)−C(14)	1.946(46)	C(14)−B(19)	1.608(63)	B(20)−Cs(1A)	3.729(45)
Cs(1)−B(21A)	3.751(52)	C(11)−B(15)	1.653(63)	C(14)−B(21)	1.585(66)	B(21)−B(22)	1.615(65)
Cs(1)−C(35A)	3.574(60)	C(11)−B(17)	1.672(67)	C(14)−B(22)	1.509(59)		
			Compound **VIII**				
Si(1)−C(11)	1.847(17)	B(12)−C(13)	1.668(37)	B(15)−B(21)	1.530(56)	B(19)−C(20)	2.016(37)
Si(4)−C(17)	1.867(19)	B(12)−B(18)	1.835(44)	B(16)−C(17)	1.634(30)	C(20)−B(21)	1.704(32)
Si(3)−C(20)	1.832(15)	C(13)−B(14)	1.693(30)	B(16)−B(21)	1.808(36)	C(20)−B(22)	1.758(35)
Si(2)−C(13)	1.803(17)	C(13)−B(18)	1.727(37)	B(16)−B(22)	1.795(35)	B(21)−B(22)	1.781(40)
C(11)−B(12)	1.629(36)	C(13)−B(19)	1.750(44)	C(17)−B(18)	1.690(37)	Li−O(51)	1.926(36)
C(11)−B(15)	1.810(48)	B(14)−B(15)	1.701(53)	C(17)−B(19)	1.731(46)	Li−O(61)	1.956(35)
C(11)−B(16)	1.732(30)	B(14)−C(20)	1.737(31)	C(17)−B(22)	1.614(35)	Li−O(71)	1.945(32)
C(11)−B(21)	1.691(32)	B(15)−C(20)	1.809(50)	B(18)−B(19)	1.868(44)	Li−O(81)	1.841(35)
			Compound **XI**				
Mg−C(11)	2.304(7)	Si(2)−C(18)	1.890(6)	C(14)−B(19)	1.581(9)	C(17)−B(21)	1.750(10)
Mg−B(13)	2.670(9)	C(11)−B(12)	1.680(9)	C(14)−B(20)	1.596(11)	C(17)−C(41)	1.569(10)
Mg−B(15)	2.345(8)	C(11)−B(13)	1.529(9)	B(15)−B(16)	1.775(11)	C(18)−B(19)	1.585(10)
Mg−B(16)	2.385(8)	C(11)−B(15)	1.693(10)	B(15)−B(22)	1.728(10)	C(18)−B(21)	1.719(11)
Mg−C(17)	2.394(6)	C(11)−C(37)	1.548(8)	B(16)−C(17)	1.625(10)	C(18)−B(22)	1.687(10)
Mg−B(20)	2.800(7)	B(12)−B(15)	1.769(11)	B(16)−B(21)	1.822(10)	B(19)−B(20)	2.046(12)
Mg−N(51)	2.164(6)	B(12)−C(18)	1.682(9)	B(16)−B(22)	1.762(12)	B(19)−B(21)	2.079(12)
Mg−N(52)	2.205(6)	B(12)−B(22)	1.780(11)	C(17)−B(20)	1.531(11)	B(21)−B(22)	1.775(11)
Si(1)−C(14)	1.868(6)	B(13)−C(14)	1.565(9)				
			Compound **XII**				
Mg−B(5)	2.468(5)	C(3)−B(8)	1.596(6)	C(4)−B(12)	1.669(6)	B(7)−B(8)	1.746(7)
Mg−B(6)	2.387(5)	C(3)−B(9)	1.801(6)	B(5)−B(6)	1.822(7)	B(7)−B(10)	1.759(6)
Si(1)−C(3)	1.847(4)	C(3)−B(10)	1.695(5)	B(5)−B(7)	1.810(6)	B(7)−B(11)	1.787(7)
Si(2)−C(4)	1.859(4)	Mg−B(7)	2.506(5)	B(5)−B(8)	1.850(7)	B(8)−B(10)	1.798(7)
C(1)−C(2)	1.332(5)	Mg−O(31)	2.026(3)	B(6)−B(7)	1.776(6)	B(9)−B(12)	1.851(6)
C(1)−B(9)	1.559(6)	C(3)−B(12)	1.657(6)	B(6)−B(11)	1.778(6)	B(10)−B(11)	1.779(7)
C(1)−C(21)	1.520(5)	C(4)−B(6)	1.577(6)	Mg−O(41)	2.044(3)	B(10)−B(12)	1.749(7)
C(2)−B(5)	1.607(5)	C(4)−B(9)	1.770(6)	Mg−O(51)	2.012(3)	B(11)−B(12)	1.743(6)
C(2)−C(22)	1.514(6)	C(4)−B(11)	1.701(6)				

Table 2 (Continued)

Bond Angles (deg)							
Compound IV							
C(11)−Mg−C(16)	96.6(2)	B(12)−C(11)−B(13)	115.6(5)	B(15)−C(14)−B(20)	65.6(3)	B(17)−C(18)−B(19)	110.7(4)
O(51)−Mg−O(61)	102.8(1)	C(11)−B(12)−C(18)	128.0(4)	B(19)−C(14)−B(20)	64.8(4)	B(15)−B(22)−C(16)	56.3(3)
Mg−C(11)−B(12)	91.6(3)	C(11)−B(13)−C(14)	126.2(5)	B(12)−C(18)−B(17)	92.9(3)	C(16)−B(22)−B(17)	56.3(3)
Mg−C(11)−B(13)	90.3(3)						
Compound V							
C(11)−Mg−B(15)	41.7(1)	B(13)−C(11)−B(15)	134.9(3)	C(11)−B(15)−B(16)	117.7(3)	C(14)−B(19)−C(18)	121.7(3)
B(15)−Mg−B(16)	44.3(1)	C(11)−B(12)−C(18)	120.9(2)	B(15)−B(16)−C(17)	119.9(3)	B(20)−B(19)−B(21)	81.5(2)
B(16)−Mg−C(17)	41.1(1)	C(11)−B(13)−C(14)	128.1(4)	B(16)−C(17)−B(20)	135.9(3)	C(14)−B(20)−C(17)	125.2(3)
O(51)−Mg−O(61)	91.1(1)	B(13)−C(14)−B(20)	112.0(3)	B(12)−C(18)−B(19)	114.4(3)	C(17)−B(20)−B(19)	89.6(3)
Compound VI							
C(11)−Mg−B(15)	41.9(4)	B(12)−C(11)−B(13)	99.8(8)	B(13)−C(14)−B(19)	111.7(8)	B(15)−B(16)−C(17)	119.1(8)
B(15)−Mg−B(16)	44.4(4)	B(13)−C(11)−B(15)	133.5(8)	B(13)−C(14)−B(20)	112.4(8)	C(14)−B(19)−C(18)	123.3(9)
B(16)−Mg−C(17)	40.8(4)	C(11)−B(13)−C(14)	129.9(9)	C(11)−B(15)−B(16)	118.8(8)	C(14)−B(20)−C(17)	129.5(9)
Compound VII							
C(11)−Cs(1)−B(15)	26.9(10)	C(12)−Cs(1)−B(16)	27.5(11)	C(13)−Cs(1)−B(17)	26.1(13)	C(13)−Cs(1)−B(16A)	147.7(12)
C(12)−Cs(1)−B(15)	27.0(12)	C(13)−Cs(1)−B(16)	30.5(11)	C(11)−Cs(1)−B(16A)	140.3(11)	B(15)−Cs(1)−B(16A)	150.9(12)
C(13)−Cs(1)−B(15)	55.4(12)	C(11)−Cs(1)−B(17)	27.7(11)	C(12)−Cs(1)−B(16A)	157.8(11)	B(16)−Cs(1)−B(16A)	165.2(2)
C(11)−Cs(1)−B(16)	53.6(10)						
Compound VIII							
B(12)−C(11)−B(15)	95.5(20)	B(14)−C(13)−B(18)	130.0(17)	C(11)−B(16)−C(17)	108.4(15)	C(20)−B(22)−B(21)	57.6(14)
B(12)−C(11)−B(16)	107.1(17)	B(14)−C(13)−B(19)	77.5(16)	B(19)−C(17)−B(22)	79.5(17)	O(51)−Li−O(61)	101.1(16)
C(11)−B(12)−C(13)	112.9(20)	C(13)−B(14)−B(15)	106.7(21)	C(13)−B(19)−C(20)	94.6(18)	O(51)−Li−O(71)	108.7(16)
C(11)−B(12)−B(18)	102.9(21)	C(13)−B(14)−C(20)	107.9(16)	C(17)−B(19)−C(20)	93.3(18)	O(51)−Li−O(81)	109.3(17)
B(12)−C(13)−B(14)	101.6(16)	C(11)−B(15)−B(14)	107.6(25)	B(15)−C(20)−B(22)	109.0(19)		
Compound XI							
C(11)−Mg−B(15)	42.7(3)	B(13)−C(14)−B(19)	111.1(5)	N(51)−Mg−N(52)	81.9(2)	C(14)−B(19)−B(21)	112.1(5)
B(16)−Mg−C(17)	39.8(2)	B(13)−C(14)−B(20)	117.7(5)	B(12)−C(11)−B(13)	100.7(5)	B(20)−B(19)−B(21)	71.0(4)
B(13)−C(11)−B(15)	132.9(5)	C(11)−B(15)−B(16)	119.2(5)	B(16)−C(17)−B(20)	134.0(6)	C(17)−B(20)−B(19)	100.7(5)
C(11)−B(13)−C(14)	129.5(6)	B(15)−B(16)−C(17)	121.6(6)	B(12)−C(18)−B(19)	114.2(5)	C(17)−B(21)−B(19)	92.4(5)
Compound XII							
C(2)−C(1)−B(9)	118.5(3)	B(8)−C(3)−B(12)	114.9(3)	C(4)−B(6)−B(5)	112.1(3)	C(3)−B(9)−C(4)	96.2(3)
C(2)−C(1)−C(21)	123.2(4)	B(6)−C(4)−B(11)	65.6(3)	B(6)−B(7)−B(8)	106.6(3)	C(1)−B(9)−B(12)	151.2(3)
B(9)−C(1)−C(21)	118.4(3)	B(9)−C(4)−B(11)	117.0(3)	B(10)−B(7)−B(11)	60.2(3)	B(11)−B(10)−B(12)	59.2(3)
C(1)−C(2)−B(5)	120.0(3)	C(2)−B(5)−B(7)	146.4(3)	C(3)−B(8)−B(5)	111.0(3)	C(4)−B(11)−B(6)	53.9(2)
C(1)−C(2)−C(22)	123.2(3)	B(6)−B(5)−B(7)	58.6(2)	C(1)−B(9)−C(3)	110.3(3)	B(6)−B(11)−B(7)	59.8(3)
B(5)−C(2)−C(22)	116.8(3)	B(6)−B(5)−B(8)	100.5(3)	C(1)−B(9)−C(4)	111.0(3)	B(10)−B(11)−B(12)	59.6(3)
B(8)−C(3)−B(9)	109.7(3)						

C(17) = 2.326(9) Å, with the next nearest neighbor cage atom distances being Mg−B(13) = 2.644(12) Å and Mg−B(20) = 2.687(14) Å; compounds **V** and **X** show similar distances. These distances are comparable to the Mg−cage atom distances found in the slip-distorted half-sandwich magnesacarborane dimer [*closo*-1-Mg(TMEDA)-2,3-($SiMe_3$)$_2$-2,3-$C_2B_4H_4$]$_2$, which range from a Mg−C_{cage} distance of 2.649(3) Å to a Mg−B_{unique} distance of 2.393(3) Å,[26] and those found in *closo*-1-Mg(THF)$_3$-2,4-($SiMe_3$)$_2$-2,4-$C_2B_4H_4$ (range 2.381(4)−2.452(3) Å).[27] An inspection of the nearest neighbor B−C_{cage} distances in compounds **V**, **VI**, and **XI** reveals very uneven intracage bonding (see Table 2). On the basis of bond distances, atoms B(13) and C(14) seem to be electron-precise, while the other atoms are involved in an electron deficient $(CR)_3B_7H_9$ fragment. The average B(13)−C(11) bond distance is 1.542 ± 0.009 Å, and the B(13)−C(14) distance is 1.561 ± 0.007 Å, while the next closest cage atoms, B(12), B(19), and B(20), are over 2.5 Å away. In the same way, the three nearest neighbor distances to C(14) are 1.561 ± 0.007, 1.587 ± 0.010, and 1.583 ± 0.009 Å for B(13), B(19), and B(20), respectively, with the next closest atoms (C(11) and C(18)) being at distances of over 2.7 Å. It should be pointed out that this division is somewhat arbitrary; while the electron-precise label for B(13) and C(14) is well-substantiated in the structure, the immediate bonding environments of boron atoms B(19) and B(20) are more difficult to describe. As with B(13), these boron atoms form two strong bonds with their neighboring cage carbons, but their next nearest neighbor distances are ∼2 Å, which puts them on the borderline of what could be considered as "normal" B−B cage bond distances. The solid-state structure of the B-Me substituted magnesacarborane, $(THF)_2Mg(SiMe_3)_4(BMe)C_4B_7H_7$ (**IV**), shown in Figure 1, is different from those of the other three "carbons adjacent" magnesacarboranes. As with **V**, **VI**, and **XI**, the carborane cage can be divided into an electron-precise segment consisting of B(12), B(13), and C(11), bonded to an electron-deficient $(CSiMe_3)_3(BMe)B_5H_5$ cage. The nine-vertex cage is similar in structure to the *arachno*-carborane 1,3-$C_2B_7H_{13}$, if the $Me_3SiC(16)$ unit is replaced by a BH group with two bridged hydrogens.[28] The Mg atom is strongly bonded to C(17) and C(11) and can be considered as η^2-bonded to the cage. To ascertain the extent of the structural influence exerted by the magnesium groups, the geometries of model dianions, $[C_4B_8H_{12}]^{2-}$ (**IV′** and **VI′**), were optimized at the B3LYP/6-31G* level of theory, starting with the cage geometries

(26) Hosmane, N. S.; Zhu, D.; McDonald, J. E.; Zhang, H.; Maguire, J. A.; Gray, T. G.; Helfert, S. C. *Organometallics* **1998**, *17*, 1426.
(27) Zheng, C.; Wang, J.-Q.; Maguire, J. A.; Hosmane, N. S. *Main Group Met. Chem.* **1999**, *22*, 361.
(28) (a) Tebbe, F. N.; Garrett, P. M.; Hawthorne, M. F. *J. Am Chem. Soc.* **1966**, *88*, 607. (b) Voet, D.; Lipscomb, W. N. *Inorg. Chem.* **1967**, *6*, 113.

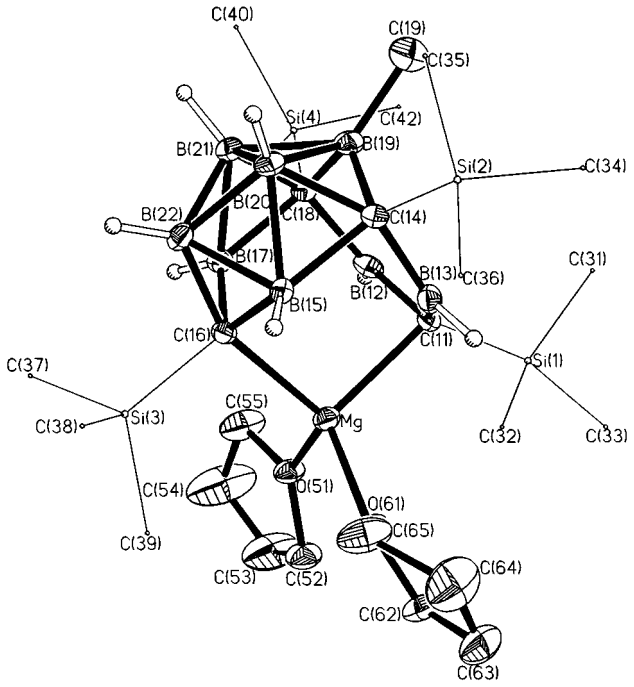

Figure 1. Crystal structure of $(THF)_2Mg(SiMe_3)_4(B\text{-}Me)\text{-}C_4B_7H_7$ (**IV**) showing the atom-numbering scheme. The thermal ellipsoids are drawn at the 40% probability level. For clarity, the H atoms of the methyl and methylene moieties are omitted and the $SiMe_3$ groups are drawn with circles of arbitrary radii.

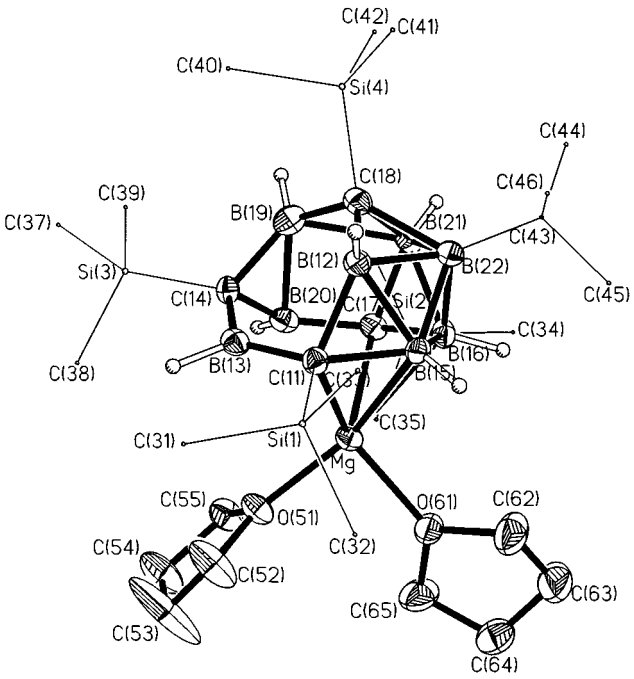

Figure 2. Perspective view of $(THF)_2Mg(SiMe_3)_4(B\text{-}t\text{-}Bu)\text{-}C_4B_7H_7$ (**V**) showing the atom-numbering scheme. The thermal ellipsoids are drawn at the 40% probability level. For clarity, the B_{cage}-bound *tert*-butyl group and the C_{cage}-bound $SiMe_3$ groups are drawn with circles of arbitrary radii, and the THF H's are omitted.

of **IV** and **VI**, respectively. The results are summarized in Table 3. A comparison of the equivalent distances in Tables 2 and 3 shows very good agreement between the calculated and observed distances; for **V′** the average difference is ±0.017 Å, with a maximum of 0.035 Å for

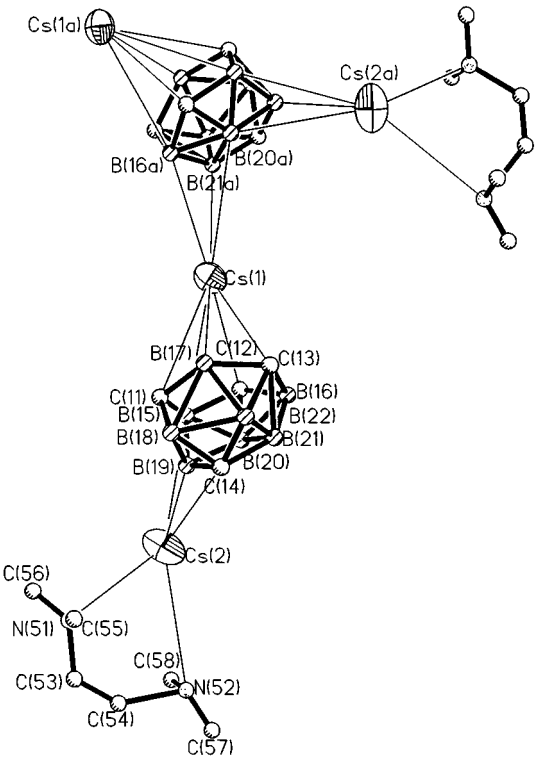

Figure 3. Crystal structure of $[exo\text{-}Cs(TMEDA)\text{-}1\text{-}Cs\text{-}(SiMe_3)_4C_4B_8H_8]_n$ (**VII**) showing the atom-numbering scheme. For clarity, all H atoms and the C_{cage}-bound $SiMe_3$ groups are omitted.

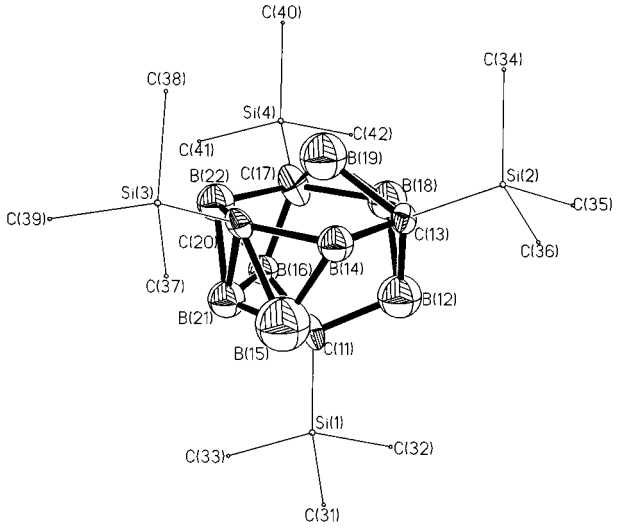

Figure 4. Crystal structure of $[(THF)_4Li][(SiMe_3)_4C_4B_8\text{-}H_9]$(**VIII**) without the exo-polyhedral $Li^+(THF)_4$ unit, showing the atom-numbering scheme. The thermal ellipsoids are drawn at the 40% probability level. For clarity, the C_{cage}-bound $SiMe_3$ groups are drawn with circles of arbitrary radii, and all H's are omitted.

the C(14)−B(19) distance. In **VI′** the average deviation was ±0.030 Å, with a maximum of 0.073 Å for B(16)−C(17) distance. These results indicate that the metal does not materially affect cage geometry. The calculated energies of **IV′** and **VI′** are essentially the same (ΔE for the transformation **VI′** to **IV′** was −1.2 kJ/mol). Both theory and experiment indicate that the situation in the "carbons apart" magnesacarborane system is one in which a number of nearly energy equivalent isomers can

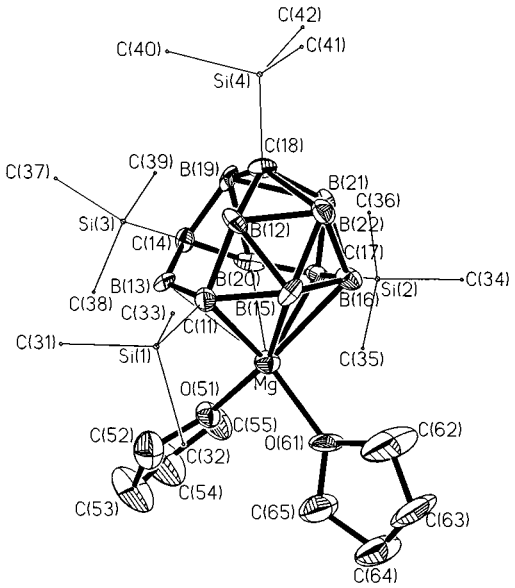

Figure 5. Crystal structure of $(THF)_2Mg(SiMe_3)_4C_4B_8H_8$ (**VI**) showing the atom-numbering scheme. The thermal ellipsoids are drawn at the 40% probability level. For clarity, all H atoms are omitted and the C_{cage}-bound $SiMe_3$ groups are drawn with circles of arbitrary radii.

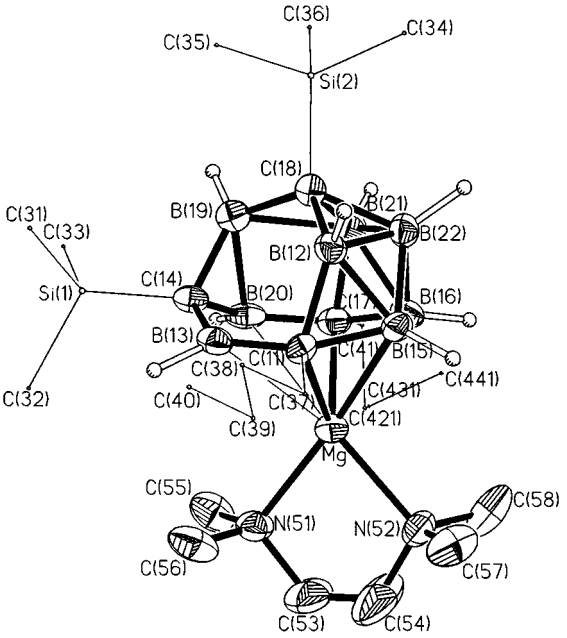

Figure 6. Crystal structure of $(TMEDA)Mg(SiMe_3)_2(n\text{-}Bu)_2C_4B_8H_8$ (**XI**) showing the atom-numbering scheme. The thermal ellipsoids are drawn at the 40% probability level. For clarity, the H atoms of the TMEDA group are omitted, and the C_{cage}-bound *n*-butyl and $SiMe_3$ groups are drawn with circles of arbitrary radii.

coexist in equilibrium and be trapped by the metal ion. Any solid product collected could just as well be dictated by kinetics and/or differential solubility as by thermodynamic stability. The fact that the solution ^{11}B NMR spectra of **IV** and **V** are the same despite their having different solid-state structures is consistent with such a description. The only "carbons adjacent" magnesacarborane synthesized and characterized in this study is *exo*-$(\mu\text{-}H)_3Mg(THF)_3(SiMe_3)_2(Me)_2C_4B_8H_8$ (**XII**), the structure of which is shown in Figure 7. As can be seen, the Mg atom is located well outside of the cage so that

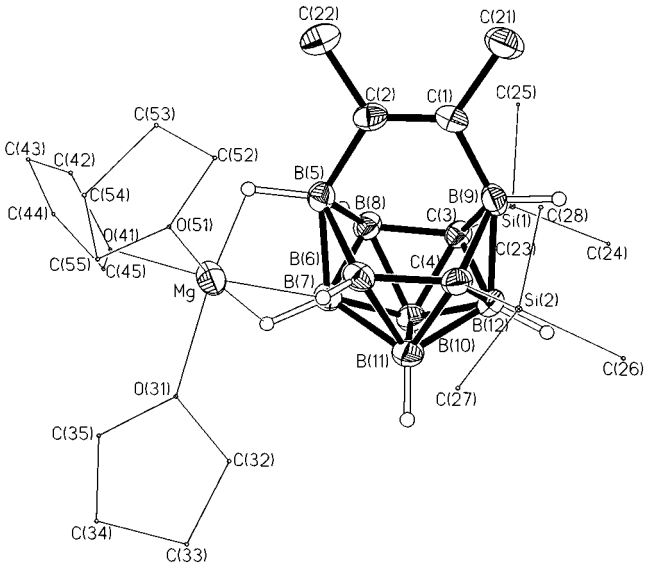

Figure 7. Crystal structure of *exo*-$(\mu\text{-}H)_3Mg(THF)_3(SiMe_3)_2(Me)_2C_4B_8H_8$ (**XII**) showing the atom-numbering scheme. The thermal ellipsoids are drawn at the 40% probability level. For clarity, the H atoms of the C_{cage}-bound Me group are omitted, and the C_{cage}-bound $SiMe_3$ groups and Mg-bound THF's are drawn with circles of arbitrary radii.

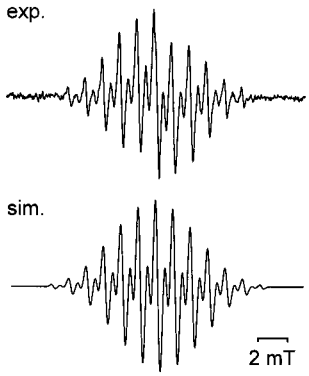

Figure 8. EPR spectrum (top) and computer simulation (bottom) of the intermediate during the reduction of $(SiMe_3)_4C_4B_8H_8$ with lithium metal in THF at room temperature.

Table 3. B3YLP/6-31G* Optimized Bond Distances (Å) for the Dianions IV′ and VI′

Compound **IV′** [a]					
C(11)−B(12)	1.482	C(14)−B(19)	1.656	C(18)−B(17)	1.728
C(11)−B(13)	1.482	B(15)−B(20)	1.835	B(19)−B(20)	1.783
B(12)−C(18)	1.619	B(15)−B(22)	1.867	B(19)−B(21)	1.782
B(13)−C(14)	1.618	C(16)−B(22)	1.628	B(20)−B(21)	1.747
C(14)−B(15)	1.728	B(17)−B(22)	1.867	B(20)−B(22)	1.772
Compound **VI′** [b]					
C(11)−B(12)	1.632	B(13)−C(14)	1.553	C(17)−B(20)	1.511
C(11)−B(13)	1.518	C(14)−B(19)	1.578	C(17)−B(21)	1.720
C(11)−B(15)	1.655	C(14)−B(20)	1.608	C(18)−B(19)	1.561
B(12)−B(15)	1.786	B(15)−B(16)	1.783	C(18)−B(21)	1.733
B(12)−C(18)	1.692	B(15)−B(22)	1.744	C(18)−B(22)	1.714
B(12)−B(22)	1.745	B(16)−C(17)	1.571	B(21)−B(22)	1.809

[a] Atom-numbering system given in Figure 1. [b] Atom-numbering system given in Figure 2.

the compound can be considered as being composed of a $[(THF)_3Mg]^{2+}$ cation that is loosely associated with a $[(SiMe_3)_4C_4B_8H_8]^{2-}$ anion. As with **IV**−**VI** and **XI**, the carborane seems to have both an electron-deficient part (an *arachno*-$(SiMe_3)_2C_2B_8H_8$ fragment) and an electron-

precise part, an ethene fragment, consisting of C(1) and C(2). The *arachno* cage is similar in structure to the *arachno*-6,9-$C_2B_8H_{14}$ cage, when C(3) and C(4) in Figure 7 are exchanged with B(5) and B(9).[29]

Different structures were also found for the group 1 metallacarboranes **VII** and **VIII**, as shown in Figures 3 and 4, respectively. The cesiacarborane **VII** crystallizes as a polymeric structure in which one cesium occupies an apical position above an open six-membered C_3B_3 face (Cs(1)−C(11,12,13) = 3.5(4), 2.95(4), 3.51(5) Å; Cs(1)−B(15,16,17) = 3.53(5), 3.56(5), 3.32(6) Å) and also bonds to a B_3 face of a neighboring carborane through a set of three unequal Cs−H−B bonds (Cs(1)−B(16a,20a,21a) = 3.44(5), 3.73(4), 3.75(5) Å) (Figure 3). The net effect is a staggered $-C_4B_8-Cs-C_4B_8-Cs-$ polymeric structure. There is an additional TMEDA-solvated Cs that is not part of the polymeric structure but is attached to each cage via upper- and lower-belt M−H−E interactions (where E = B, C) (Cs(2)−B(15,-19,20) = 3.70(5), 3.53(5), 3.75(4) Å; Cs(2)−C(34) = 3.64-(4) Å) (Figure 3). The primary six-membered C_3B_3 faces of the carboranes are not planar but show that one carbon, C(12), and one boron, B(17), are displaced toward the capping Cs (see Figure 3). However, the other Cs−C_3B_3 distances indicate considerable metal interactions with all of the facial atoms, so that the capping Cs atoms could be considered to be η^6-bonded to the cage. It should be noted that the structure of the dianion cage in **VII** is quite different from those found in the magnesacarboranes **IV**−**VI** and **XI**. In contrast to the polymeric structure found in **VII**, the lithiacarborane $[(THF)_4Li][(SiMe_3)_4C_4B_8H_9]$ (**VIII**) is monomeric, with a single THF-solvated metal ion interacting only weakly, if at all, with the carborane cage (see Figure 4 without the Li metal). Compound **VIII** is the final product of a sequence of reactions between the alkali metal and the carborane, with a paramagnetic intermediate, thought to be a $[(SiMe_3)_4C_4B_8H_8]^-$ monoanion, being initially formed. The intermediate reacts with a second equivalent of Li, producing the diamagnetic dianion $[(SiMe_3)_4C_4B_8H_8]^{2-}$, which on protonation gives $[(THF)_4Li][(SiMe_3)_4C_4B_8H_9]$. At present it is not possible to determine either the source or the location of the proton. However, theoretical calculations on various protonated species at the B3LYP/6-31G* level indicate that protonation most likely occurs at the bridging positions between B(12)−B(18) or B(14)−B(15), rather than on one of the cage carbons. However, the results are by no means conclusive and the formulation of compound **VIII** still must be based essentially on its diamagnetism and its chemical analysis.

Spectroscopy. The structures of the magnesacarboranes **IV**−**VI** and **XI** show the division of the carborane cages into electron-precise and electron-deficient fragments. Therefore, the shieldings of the boron and carbon atoms in the two fragments should be quite different, with the electron-precise atoms being less shielded than those found in the electron-deficient cage fragments. Borons B(13) in **V**, **VI**, and **XI** and B(12) and B(13) in **IV** have bonding environments similar to that found in $(CH_3)_3B$ and should have similar chemical shifts in their ^{11}B NMR spectra. The ^{11}B NMR resonance for $(CH_3)_3B$ has been reported by a number of investigators to be in the δ 84−87 ppm range.[32] This agrees quite well with a δ value of 84.3 ppm calculated for the compound at the GIAO-B3LYP/6-31G* level on the B3LYP/6-31G* optimized structure. These same calculations predict δ values in the 60−70 ppm range for the electron-precise borons in magnesacarboranes. A review of the ^{11}B NMR spectra listed in the Experimental Section shows that all δ values are negative. This is strong additional evidence that in solution the group 1 and 2 tetracarbon carboranes are fluxional or exist in a number of isomeric forms. This same situation was found for the neutral C_4B_8 precursors, as well as the "carbons adjacent" compounds studied by Grimes.[1] Therefore, although NMR spectra can be obtained for all the tetracarbon metallacarboranes, they are of limited use in their structural determinations.

Summary. The reaction of the "carbon apart" C_4B_8 carboranes with several group 1 metals and a group 2 metal (Mg) produced metallacarboranes with a variety of cage structures. Two types of cages were found for the magnesacarboranes, one depicted in Figure 1 for $(THF)_2Mg(SiMe_3)_4(B\text{-}Me)C_4B_7H_7$ (**IV**) and the other shown in Figures 2, 5, and 6 for $(L)_2Mg(SiMe_3)_2(R)_2(B\text{-}Y)C_4B_7H_7$ (L = THF, R = $SiMe_3$, Y = *t*-Bu (**V**); L = THF, R = $SiMe_3$, Y = H (**VI**); $(L)_2$ = TMEDA, R = *n*-Bu, Y = H (**XI**)). Both cages are characterized by the presence of both electron-precise boron and carbon atoms, as well as electron-deficient carborane fragments. This cage division is probably the result of two competing structure-defining factors: the cage electron-pair count and the tendencies of the more electronegative carbons to preferentially bond to boron atoms and occupy low-coordination sites.[33] At present, it is not possible to predict what isomer will form in a particular reaction. Ab initio molecular orbital calculations indicate that the two cages have equivalent energies. In addition, the solution ^{11}B NMR spectra of **IV** and **V** are the same, despite the two compounds having different solid-state structures. It seems likely that equilibrium mixtures of the two isomers, as well as others, exist in solution which may be trapped by the metal group. Under such circumstances, factors such as solubility, rather than cage stability, may be important in determining the structure of the isolated solid product. Different cage products were also observed from the reaction of the "carbons apart" C_4B_8 carboranes with group 1 metals. These reactions proceed in two distinct steps, one involving the formation of a paramagnetic intermediate, presumably the $[(SiMe_3)_4C_4B_8H_8]^-$ monoanion, which then further reacts with another equivalent of metal to give a diamagnetic C_4B_8 dianion. The final products for the lighter group 1 metals are the protonated compounds $[(THF)_4M][(SiMe_3)_4C_4B_8H_9]$ (M = Li (**VIII**), Na (**IX**), K (**X**)), while the reaction with Cs gives a polymeric

(29) Stibr, B.; Plesek, J.; Hermánek, S. In *Advances in Boron and the Boranes*; Liebman, J. F., Greenberg, A., Williams, R. E., Eds., VCH: New York, 1984; Chapter 3.

(30) Tolpin. E. I.; Lipscomb, W. N. *Inorg. Chem.* **1973**, *12*, 2257.

(31) Churchill, M. R.; DeBoer, B. G. *Inorg. Chem.* **1973**, *12*, 2674.

(32) Eaton, G. R.; Lipscomb, W. N. *NMR Studies of Boron Hydrides and Related Compounds*; W. A. Benjamin: New York, 1969, and references therein.

(33) Williams, R. E. In *Electron Deficient Boron and Carbon Clusters*; Olah, G. A., Wade, K., Williams, R. E., Eds.; Wiley-Interscience: New York, 1991; Chapter 2.

product containing two Cs atoms for every dianionic C_4B_8 carborane.

Acknowledgment. This work was supported by grants from the donors of the Petroleum Research Fund, administered by the American Chemical Society, the Robert A. Welch Foundation (Grant Nos. N-1016 & N-1322), the National Science Foundation, and funds from Northern Illinois University.

Supporting Information Available: Atomic coordinates (Table S-1), all bond lengths and bond angles (Table S-2), anisotropic displacement parameters (Table S-3), and H atom coordinates and isotropic displacement coefficients (Table S-4) for **IV**−**VIII**, **XI**, and **XII**. This material is available free of charge via the Internet at http://pubs.acs.org.

OM990677Z